SOVIET PHYSICS JETP VOLUME 11, NUMBER 2 AUGUST, 1960

# *ENERGY DISTRIBUTION OF SPUTTERED AND SCATTERED IONS IN THE BOMBARDMENT OF TANTALUM AND MOLYBDENUM BY POSITIVE CESIUM IONS*

V. I. VEKSLER

Central Asia State University

Submitted to JETP editor June 30, 1959

J. Exptl. Theoret. Phys. (U.S.S.R.) **38**, 324-334 (February, 1960)

A method is described for studying the energy spectra of scattered and sputtered ions produced in the bombardment of metals by positive ions. The energy spectra of the $Cs^+$, $Mo^+$, and $Ta^+$ ions obtained by bombarding molybdenum and tantalum targets ($T \sim 1600 - 1800°K$) with $Cs^+$ ions with energies $U = 900 - 2150$ ev have been investigated. The sputtering and scattering components have been separated from the secondary-emission ion spectra which have been described earlier; the result is a considerable reduction in the limiting energy in the spectrum of $Cs^+$ scattered on molybdenum. The width of the energy spectrum for the sputtered ions is found to be 30 — 35 ev for $Mo^+$ and 35 — 50 ev for $Ta^+$; these values are much higher than the value of 5 ev which is quoted in the literature. These results indicate that the probability of ionization of a sputtered atom which escapes from the surface increases as its energy increases.

THE energy distributions of scattered secondary ions which arise in the bombardment of surfaces by accelerated positive ions have been studied by many authors.[1-4] However, the energy distributions of the ions which are emitted in cathode sputtering of surfaces have not been investigated to any great extent, although this process has been studied recently by a number of workers.[5-8] This situation is a result of the difficulty of the required experimental techniques and the fact that a mass-spectroscopic analysis is needed. Honig[7] has studied the energy distributions of $Ge^+$ and $Na^+$ ions ejected from the surface of a non-degassed single germanium crystal and reports that at primary-ion energies of $U = 100 - 400$ ev the maximum in the distribution occurs at an energy of the order of 2 ev, although there is a considerable number of ions with energies of the order of 10 — 12 ev. Bradley[8] has estimated the width of the energy distribution for $Mo^+$ ions sputtered from a molybdenum surface from the shape of the $Mo^+$ peak of a mass spectrometer measurement and reports a value of the order of 5 ev ($U \sim 500$ ev). This author concludes that the ionization probability is higher for slower sputtered atoms.

In the work described by Honig[7] and Bradley[8] there is no indication that account has been taken of the variation in transmission of the mass spectrometer with changing initial ion energy; this effect can lead to appreciable distortion of the ion energy distribution (the main distortion is an exaggeration of the number of high-energy ions). An analysis of the operation of the instruments in question indicates that this distortion effect is more important in the work reported by Bradley than in that reported by Honig. Thus, at the present time there are no reliable data on the energy distributions of the ions produced in cathode sputtering. This problem is of interest from the point of view of obtaining information concerning the energy distributions of neutral particles produced in cathode sputtering as well as accumulating information on the nature of electron exchange in the interaction of a slowly moving atom with the surface of a material (effects which are probably different for metals and semi-conductors). There are also certain contradictions in the data on scattering of ions from metallic surfaces.

In the present work we describe an investigation of the energy spectra of different ion-emission components, carried out by means of a method which is free from the shortcomings indicated above; results are reported on the energy distributions of sputtered and scattered ions produced in the bombardment of molybdenum and tantalum surfaces by $Cs^+$ ions.

## 1. APPARATUS AND METHOD

The complexity of the isotopic spectra of certain ions and the relatively low resolution of the mass spectrometer at our disposal made it impossible to carry out an analysis of the energy spectra with the required resolution (several electron volts) by direct examination of the shapes of ion peaks in the mass spectrometer. Hence, in addition to separating the secondary emission products by the mass spectrometer we also used an electrostatic retarding field. Appropriate tests have shown that because of scattering of the secondary ions in the mass spectrometer tube the application of a retarding field at the output of the mass analyzer causes a considerable distortion of the distribution curves. For this reason the retarding field was applied in the region in which the primary-ion target T is located (Fig. 1).

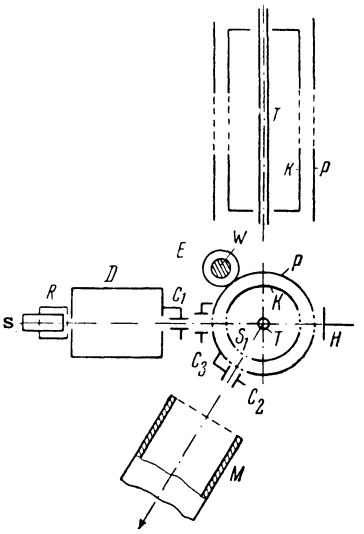

FIG. 1. Diagram of the apparatus: S – primary-ion source, S–R–D – ion gun, $C_1$, $C_2$, $C_3$ – deflection capacitors, T – target, K – cylinder of the energy analyzer, P – accelerating cylinder, M – mass-spectrometer tube, H – collector for "straight-through" ions, E – shield, W – traverse, $S_1$ – screen.

The $Cs^+$ ions obtained from the thermo-ionic source S are accelerated by a voltage applied between S and the nickel electrode D which has two longitudinal slits; these define a beam of cross section 0.4 × 5 mm. The width of the beam is estimated from the voltage applied to capacitor $C_1$, used for transverse deflection of the primary ions and to aim the primary beam on the target (a cylinder 1 mm in diameter made of molybdenum or tantalum foil 0.015 – 0.030 mm thick). The current density of the primary beam at the target was $1 - 6 \times 10^{-6}$ amp/cm². This part of the apparatus and its operation have already been described by us in detail in reference 6. The ring R, which is at a positive potential with respect to S, serves to focus the primary $Cs^+$ ions. The traversing device W, which serves as a current feed for one of the ends of the target, is surrounded by a nickel shield E. The cylinders K and P, which are shown in two projections in the figure, each have three slits which are covered by brass wire mesh with a transmission of 85% and a spacing a = 0.25 mm. The mesh is made by dipping low-transparency mesh in a 30% solution of $HNO_3$. The presence of these wire-mesh screens and the face shields on cylinder K (diameter 25 mm) prevents the penetration of the external electrostatic field into the space between T and K, in which the secondary ions are slowed down by the retarding voltage $V_0$. A voltage $V_n$ is applied between cylinders K and P; this voltage provides preliminary acceleration of the secondary ions which move toward the mass spectrometer. The total secondary-ion voltage which is applied between the cylinder K and the mass spectrometer tube M is 1250 v.

Depending on their energies, the secondary ions which leave cylinder K have different probabilities $\varphi(W)$ of passing through the mass spectrometer. The energy distribution of the secondary ions $f(W)$, the mass-spectrometer output current i, and the function $\varphi$ are related by the expression

$$i(eV_0) = e\int_{eV_0}^{\infty} f(W)\,\varphi(W - eV_0)\,dW \qquad (1)$$

which is an integral equation with kernel $\varphi(W - eV_0)$. In the method used here an approximate form of the function $\varphi(W)$ is found experimentally by plotting the dependence of the current due to the ions, which are produced by surface ionization on an incandescent target and reach the mass spectrometer detector, as a function of the voltage that accelerates these ions (between T and K). These ions can be obtained by letting a stream of neutral particles (formed when the ion source S is operated with no voltage between S and D) strike the incandescent target. It has been found subsequently (cf. below and reference 3) that at a primary-ion energy U = 2150 ev approximately 95% of the secondary $Cs^+$ ions formed at the incandescent target have energies close to thermal. It is thus possible to obtain the curves under conditions which are similar to the operating conditions (only the sign of $V_0$ is different). The values of $\varphi(W)$ obtained in both cases are found to be in good agreement. All the $\varphi(W)$ curves used for solving Eq. (1) have been obtained by the second method since it has certain advantages.

The function $\varphi(W)$ is found to be strongly dependent on both the accuracy of the adjustment of the system with respect to the tube M and the voltage $V_n$; its form was therefore investigated in all cases in which these factors were changed.

To illustrate the change in this function with changes in the voltage $V_n$, Fig. 2 shows two $\varphi(W)$ curves obtained with one of the molybdenum targets. These curves have been obtained by adjusting the TKP analyzer to achieve maximum current in the detector with minimum voltage applied to capacitor $C_2$; nevertheless, the shape of the curves indicates that the "transmission" of the mass spectrometer is quite different for ions of different energy. This result verifies the statement made in the introduction with regard to the errors which may have been introduced by Bradley.[8]

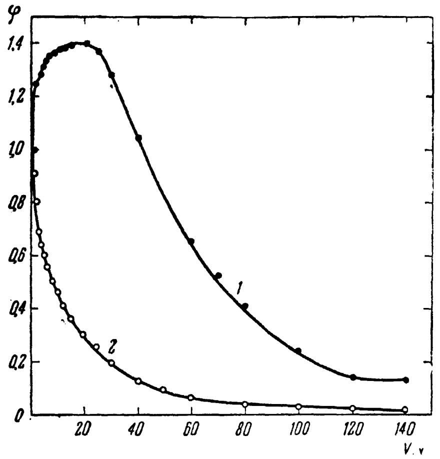

FIG. 2. The transmission of the mass spectrometer as a function of the initial energy of the ions for fixed adjustment and different values of $eV_n$: curve 1 – 100 ev, curve 2 – 250 ev.

It should be noted that the conditions under which $\varphi(W)$ is obtained by the surface ionization method (acceleration voltage applied to electrode K) differ somewhat from the conditions under which the volt-ampere characteristics are obtained in actual practice (retarding voltage applied to K). Hence, in spite of the measures taken to achieve identical conditions for the ion motion in the region T-K in both cases (cylindrical electrode system, small width of the emitting portion of the target), the effective width of the secondary ion emitter can be somewhat greater than the actual width under operating conditions. The measured results can be distorted by this effect, especially when high retarding potentials are used. Thus, some experimental method for checking the results is required. A check of this kind can be made by measuring a spectrum twice with highly different $\varphi(W)$. In Fig. 3 we show two such spectra for $Cs^+$ ions scattered on molybdenum (U = 900 ev) obtained by differentiation of the volt-ampere characteristics plotted for different values of $V_n$ (curves 1 and 2, solid points). The hollow circles and triangles denote the results obtained from solutions of the integral equation (1) corresponding to curves 1 and 2. It follows from the figure that the results obtained by solution of the integral equation (1) with the experimentally determined values of the function $\varphi(W)$ (cf. above) show considerably better agreement between themselves than the curves plotted by simple differentiation. Similar agreement of the curves is found in other cases which have been investigated ($Cs^+$ on molybdenum at U = 2150 ev with $V_n$ as the variable, $Mo^+$ at U = 2150 ev with varying alignment of the system, etc.). The distribution functions obtained by using different $\varphi(W)$ can differ by a constant; hence, in comparing these functions it is necessary to normalize the area under the f(W) curve in each case. This has been done in plotting curves shown in Fig. 3. However, in an analysis of the energy distribution of the particles there is no need for such normalization and the results given below have been obtained without normalization.

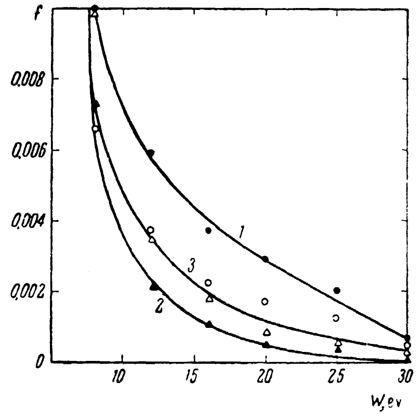

FIG. 3. Energy spectra for $Cs^+$ ions scattered on molybdenum (U = 900 ev, T = 1800°K) obtained for different functions $\varphi(W)$ and by solution of the integral equation (curve 3). Curves 1 and 2 are obtained by differentiation of the corresponding volt-ampere characteristics.

Knowing that there is a cylindrical field in the operating region T-K-P, we can estimate the variation of the potential in the region of screen $S_1$ of electrode K using a modified Maxwell formula,[9] which applies for a system of equally spaced parallel wires:

$$V \approx \frac{a}{4\pi}(\alpha V_n - \beta V_0)\ln\left(1 - 2e^{2\pi x/a}\cos(2\pi y/a) + e^{4\pi x/a}\right) + [V_0 + (V_0 + V_n)\alpha\gamma](1 + \beta x), \qquad (2)$$

where $\alpha^{-1} = r_K \ln(r_P/r_K)$, $\beta^{-1} = r_K \ln(r_K/r_T)$, $r_T$, $r_K$, $r_P$ are the radii of cylinders T, K, and P respectively; $\gamma = -(a/2\pi)\ln[2\sin\pi c/a]$, c is the radius of the wire, a is the screen spacing, x is the radial coordinate, which is measured outward from cylinder K, and y is a coordinate which is measured from the center of some wire in the direction perpendicular to the x axis of the wire. An analysis of this formula shows that the minimum

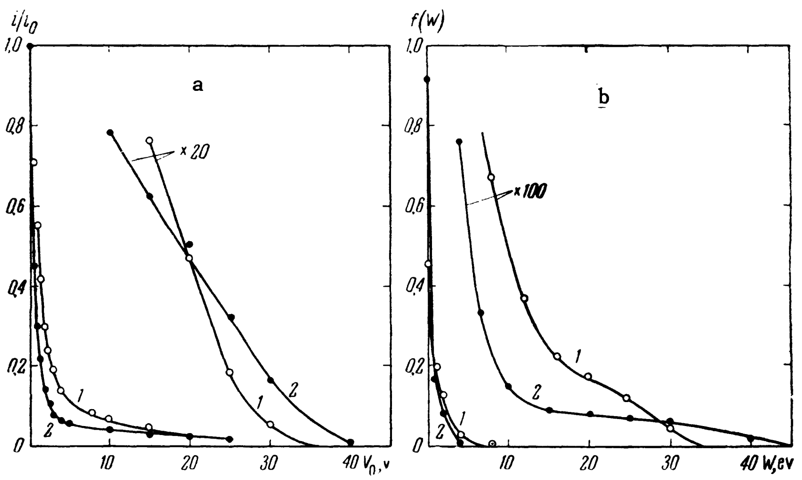

FIG. 4. Retardation curves (a) and energy spectra (b) for $Cs^+$ ions scattered on a molybdenum ($T = 1800°K$): curve 1 – $U = 900$ ev, curve 2 – $U = 2150$ ev.

departure of the potential from the potential $V_K$ of a wire in the plane $y = a/2$ is

$$\Delta V'_{min} \approx \alpha\gamma (V_0 + V_n). \quad (3)$$

Under operating conditions $V_n$ is $-100$ and $-250$ v, i.e., $\Delta V'_{min}$ with $V_0 = 0$ is respectively $-0.8$ and $-2$ v. Actually, these figures should be reduced when account is taken of the fact that wire-mesh screens are used rather than parallel wires. If, to the quantities indicated above we add the potential drop along that part of the heated target which is bombarded by ions, $\Delta V'' = 0.5$ v (the electrical system has a provision for applying the voltage $V_0$ between cylinder K and the center point of the target), we can determine the radial and angular components of the momentum in terms of energy without taking account of the contact potential, which is 1.3 v when $V_n = 100$ v and 2.5 v when $V_n = 250$ v.

The pressure of the residual gas in the apparatus is measured with an ionization gauge, while the target temperature is measured with an optical pyrometer. Before operation, the glass chamber of the instrument is heated by gas while the target is annealed for a long period of time at $T = 2300 - 2500°K$ by passing current through it. Under these conditions cylinder K is heated to 900°K by radiation while the temperature of the walls in the operating portion of the glass chamber is approximately 370°K. This outgassing procedure is continued until repeated heating of the target is no longer accompanied by a noticeable pressure rise. In operation the system is evacuated by mercury diffusion pumps and liquid-oxygen traps. The pressure by adsorption at the target with the primary ion source on was estimated by the flash method;[10] this pressure is of the order of $5 - 8 \times 10^{-8}$ mm Hg. An adsorption pressure of this order of magnitude has also been obtained by another method which we have used earlier.[11]

The currents due to secondary ions are measured by a vacuum-tube electrometer located at the output of the mass spectrometer; the sensitivity of this instrument is $5 \times 10^{-16}$ amp/mm.

The integral equation (1) can be easily reduced to the form

$$f(eV_0) = -\frac{1}{\varphi(0)}\left[\frac{di\,(eV_0)}{d\,(e^2V_0)} + \int_{eV_0}^{\infty} f(W)\,\varphi'(W - eV_0)\,dW\right]. \quad (4)$$

This equation is solved by numerical integration using an iteration method in which the first term on the right side of Eq. (4) is used as the zeroth approximation for f(W).

## 2. EXPERIMENTAL RESULTS AND DISCUSSION

The retardation curves for secondary $Cs^+$ ions obtained in the bombardment of molybdenum ($V_n = 100$ v) and tantalum ($V_n = 250$ v) targets by $Cs^+$ ions are shown in Figs. 4a and 5a respectively.* The distribution functions f(W) obtained from the retardation curves in Figs. 4a and 5a by means of Eq. (1) are shown in Figs. 4b and 5b.

In all curves obtained at high target temperatures, an especially noteworthy feature is the sharp drop of f(W) at $W \sim 1 - 2$ ev. This drop is probably due to the presence of $Cs^+$ ions among the scattered ions; these ions are produced by surface ionization of the cesium atoms which diffuse from inside the material. These atoms, in turn, are formed from $Cs^+$ ions of the primary beam which penetrate into the volume of the target. This effect has been observed earlier.[2] The energy width of this segment of the curve is found to be in agreement with the estimate of the resolving power given above.

---

*All these curves, as well as the curves in Figs. 6a and 7a (with the exception of curve 3 in Fig. 5a) are given in units of the current $i_0$ that corresponds to the curves for $V_0 = 0$. In order to facilitate a comparison with curve 1 in the same figure, curve 3 in Fig. 5a is given in units of the current $i_0$ for curve 1.

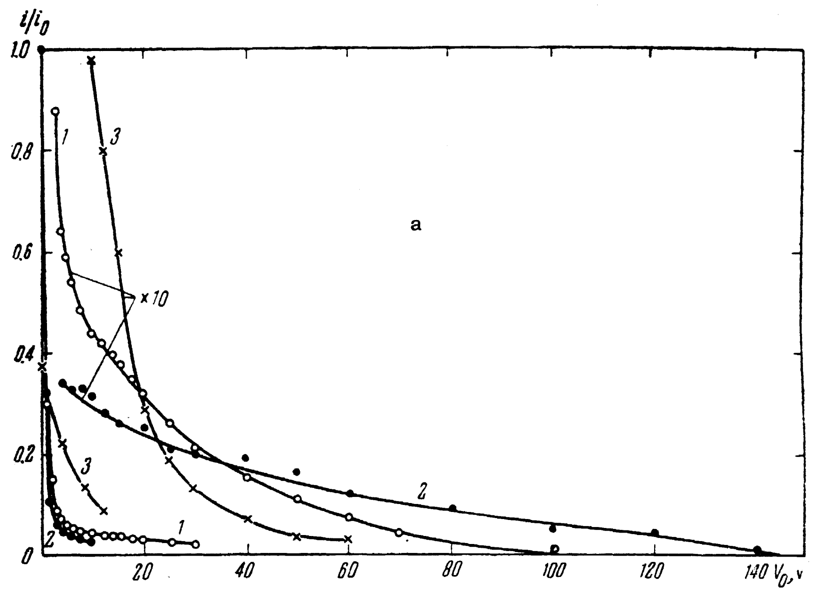

FIG. 5. Retardation curves (a) and energy spectra (b) for $Cs^+$ ions scattered on a tantalum target: curve 1 – U = 900 ev, T = 1600°K; curve 2 – U = 2150 ev, T = 1600°K; curve 3 – U = 900 ev, T ≈ 300°K.

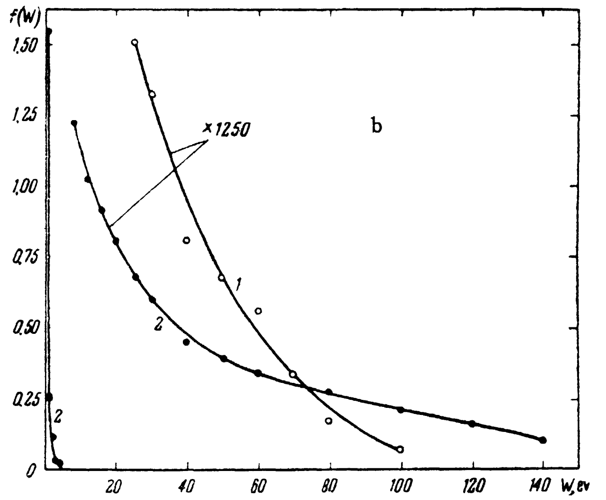

The retardation curves for $Mo^+$ and $Ta^+$ ions ejected from molybdenum and tantalum targets are given in Figs. 6a and 7a respectively.

A check on whether or not ions which enter the mass spectrometer come from the target is given by the presence of a clearly defined peak on the mass spectrogram; this peak vanishes when the primary beam is deflected from the target. The peaks corresponding to $Mo^+$ and $Ta^+$ ions are also checked by the absence of $Ta^+$ ($Mo^+$) peaks when molybdenum (tantalum) is bombarded by $Cs^+$. It should be noted that at $V_n = 250$ v and small values of $V_0$, a peak due to $Cs^+$ is partially superimposed on the $Mo^+$ peak; the $Cs^+$ ions arise as a result of bombardment of the output grid of cylinder P by scattered $Cs^+$ ions which come from the target. This situation causes a sharp drop in current on the retardation curve in the region of small $V_0$, which is characteristic of surface ionization of Cs. Hence the $Mo^+$ peak is always studied with $V_n = 100$ v.

The identification of the $Mo^+$ peak is also checked by the temperature dependence of the $Mo^+$ current (Fig. 8). At high target temperatures, in which case the surface may be assumed clean, this dependence is similar to that obtained by us earlier[5] in the bombardment of molybdenum by $Hg^+$

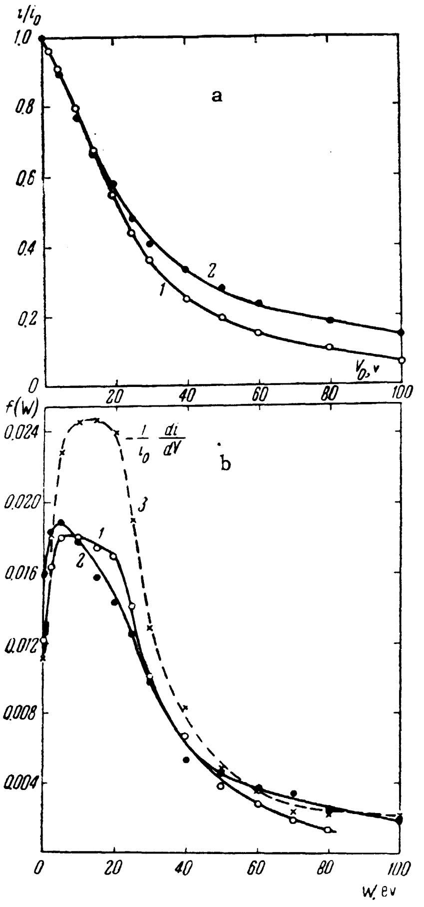

FIG. 6. Retardation curves (a) and energy spectra (b) for sputtered $Mo^+$ ions (T = 1800°K): curve 1 – U = 900 ev, curve 2 – U = 2150 ev.

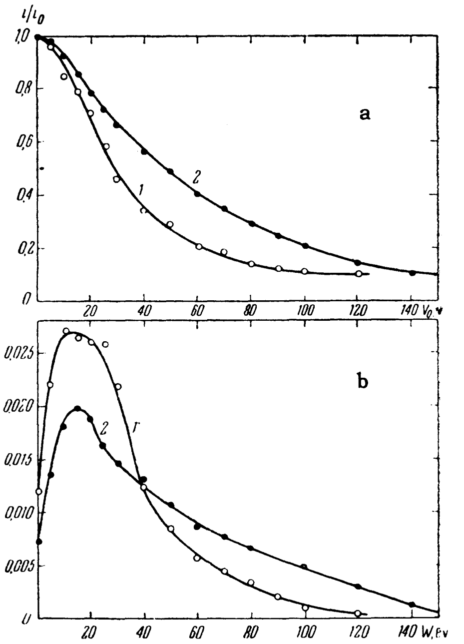

FIG. 7. Retardation curves (a) and energy spectra (b) for sputtered Ta$^+$ ions (T = 1800°K): curve 1 – U = 1200 ev, curve 2 – U = 2150 ev.

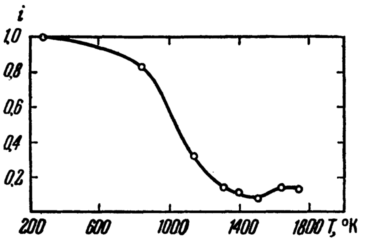

FIG. 8. The current of of sputtered Mo$^+$ ions as a function of target temperature (U = 2150 ev).

and by Bradley in the bombardment of molybdenum by Ar$^+$.$^8$

The fact that the temperature dependence of the ion component of the cathode sputtering coefficient is not affected by the nature of the bombarding ion is of interest in itself. This result indicates that the structure of the electron shell of the bombarding ion is not a factor in the sputtering of matter in the form of ions.

The energy distribution functions for Mo$^+$ and Ta$^+$ obtained from the retardation curves (Figs. 6a and 7a) by means of the integral equation (1) are shown in Figs. 6b and 7b. To demonstrate that the integral equation can be applied in this case in Fig. 6b we also show curve 3, which is obtained from curve 1 of Fig. 6a by direct differentiation. It follows from curves 1 and 3 that in the present case the correction for the change in transmission of the mass spectrometer as a function of W is small, although the position of the maximum on curve 3 is displaced toward higher energies. The reduction of this correction when the retarding-field technique is used, as compared with the analogous correction (Fig. 2) when the energy spectrum is determined from the shape of the peak at the output of the mass spectrometer, apparently results from the fact that at higher values of $V_0$ ions with a given initial energy W reach screen $S_1$ with almost zero energy and have approximately the same probability of reaching the detector of the mass analyzer.

Since the probability for surface ionization of Cs on molybdenum and tantalum is approximately 100%, the current $i_0$ (Figs. 4a and 5a) can, in a rough way, serve as a measure of the primary ion beam at the output of the mass spectrometer;$^6$ thus we can estimate the scattering coefficient $K_0$ for Cs and the sputtering coefficient $K_S$ for Mo$^+$ and Ta$^+$ (this estimate turns out to be somewhat large since we neglect scattering of cesium in the neutral state, which should have a small probability).

In the case of Cs$^+$ scattering (U = 900 ev) from a tantalum surface, $K_0$ is found to be of the order of 6% ($V_0 \geq 4$ ev) a value which is in poor agreement with the value of approximately 18% (U = 400 ev) reported by Arifov and Ayukhanov,$^2$ but in much better agreement with the data reported by Brunnee$^3$ on the reflection of Rb$^+$ ions from a molybdenum surface.

It is likely that the disagreement with the data reported by Arifov and Ayukhanov is due to the difference in the primary-ion energy in their work and the work reported here, or to the existence of noticeable anisotropy effects in the angular distribution of the scattered ions. In references 2 and 3 the scattering was averaged over all angles, whereas in the present work scattering is measured at approximately 120° with respect to the primary beam.

A comparison of curves 1 and 3 (Fig. 5a) indicates that when the surface of the equilibrium layer (T ~ 300°K) contains cesium atoms with an admixture of impurity atoms, the coefficient for secondary ion emission increases although the limiting energy of the distribution is reduced. It is possible that this phenomenon is to be associated with the sputtering of a cesium film at low temperatures, since the mean energy of the sputtered ions exceeds the mean energy of the ions obtained in surface ionization.

In cases of interaction of Cs$^+$ with a molybdenum surface, in spite of the fact that the mass m of the incident ion is greater than the mass M of the lattice atom,$^4$ it is found that the Cs$^+$ scatters on the molybdenum. The numerical value of the scattering coefficient ($K_0 \sim 4\%$ at U = 2150 ev) is of the same order of magnitude as that reported by Brunnee.$^3$ The energy spectra of the scattered ions obtained by Brunnee and by us are also similar. However, the values of the limiting energy given in Fig. 4b (approximately 40 ev) are somewhat lower than the values reported by Brunnee. It is possible that this difference is due to an angular dependence for the limiting energy or, what is more probable, the presence of sputtered ions (not taken into account in reference 3). It follows from the data of Fig. 6b that the limiting energy $W_{max}$ in sputtering of the surface is greater than 100 ev (in reference 3 the secondary ion emission components were not analyzed).

Whereas the curves in Fig. 5b indicate a proportionality between $W_{max}$ and U, as has already been observed earlier in references 1 and 3, in the scattering of $Cs^+$ from a molybdenum surface $W_{max}$ increases very slowly as U increases. This difference can be explained qualitatively as follows.

In recent papers[1-4,12] the interactions of the bombarding atoms with the lattice are treated as elastic pair collisions with atoms of the lattice. Within the framework of this analysis, scattering of the primary ion at angles greater than 90° is possible in single collisions between these ions and lattice ions only if $m < M$, in which case the limiting energy of the scattered ion that escapes from the surface is determined by the energy loss of the ion for a single pair collision. The condition $m < M$ is satisfied when $Cs^+$ scatters on a tantalum surface, in which case $W_{max}$ must be proportional to U.

In order to explain scattering of primary ions at angles greater than 90° when $m > M$ ($Cs^+$ on molybdenum) we must assume multiple collisions of these ions with the lattice atoms, owing to the increased path length of the primary ions inside the material as compared with the preceding case, to the increase in the energy loss with increasing U (for motion back to the surface), and, as a consequence, owing to the slower increase in $W_{max}$.

A further verification of this interpretation can be obtained by a comparison of the distortion of the function f(W) with increasing U in sputtering of $Mo^+$ and $Ta^+$ (cf. Figs. 6b and 7b). In one case ($Ta^+$) this distortion is essentially a change in the scale of the abscissa axis almost proportional to the energy U; because of the normalization of the distribution function this change is proportional to the reduction in the height of the curve f(W). In the case of $Mo^+$, however, there is no change in scale but the maximum of the f(W) curve is shifted toward lower energies with increasing U. It may be assumed that in the first case the formation site of the sputtered ions remains close to the surface whereas in the second case it is displaced into the material.

The width of the energy distribution of the sputtered ions corresponding to half the maximum energy of f(W) obtained in the present work (Figs. 6b and 7b) is found to be appreciably greater (30 – 35 ev for $Mo^+$ and 35 – 50 ev for $Ta^+$) than the corresponding value obtained by Bradley[8] (5 ev for $Mo^+$). A possible cause for this disagreement is discussed above. It might be thought that the recording of high-energy sputtered ions by the electrometer is subject to error because of ionization of sputtered atoms from deep inside the target which reach the spectrometer. (Ionization can be caused by thermal electrons from the target; under the present experimental conditions this electron current is of the order of one milliampere.) However, as is shown by experiments carried out at lower target temperatures and by a detailed theoretical calculation, the probability for this effect is vanishingly small. The fact that the widths of the energy distributions are about the same for the scattered and sputtered ions seems to indicate that the mechanisms for sputtering and scattering are closely related and that the transition between these phenomena is a smooth one.

The absolute value of the sputtering coefficient ($K_s \sim 2.5 \times 10^{-3}$ in the case of $Mo^+$ and $6 \times 10^{-3}$ in the case of $Ta^+$ for $U = 2150$ ev and $T = 1800°K$) agrees with the values reported in the literature.[5,6,8]

A comparison of the mean values of the energies of the neutral particles produced in cathode sputtering (15 – 20 ev, Wehner;[8] 5 – 7 ev, Sporn[13]) with the mean values of the energy of the sputtered ions (Figs. 6b and 7b) (21 – 23 ev for $Mo^+$ and 26 – 36 ev for $Ta^+$) indicates that the ionization probability for Mo and Ta atoms which escape from the surface increases as their energy increases. Support for this interpretation is also found in the fact that there is an initial increase in the function f as W increases: although the shape of the energy distribution of the neutral atoms obtained in cathode sputtering has not been investigated as yet, there are a number of indirect data (for example, the behavior of curve 3 in Fig. 5a of the present work) which indicate that the dependence is a monotonically decreasing one.

It should be noted that these facts are in qualitative agreement with the expected small (proportional to $\sqrt{W}$) increase for the ionization probability of an atom which leaves the surface of a metal as its energy increases. This increase is predicted theoretically from an analysis of electron exchange in the interaction of a slowly moving atom with the surface of a metal.[14] It would be desirable to investigate the energy spectra of sputtered neutral atoms in order to obtain a clearer picture of these phenomena.

---

[1] M. A. Eremeev, Dokl. Akad. Nauk SSSR **79**, 755 (1951). U. A. Arifov and A. Kh. Ayukhanov, Dokl. Akad. Nauk Uz. S.S.R., No. 4, 12 (1951).

[2] U. A. Arifov and A. Kh. Ayukhanov, Izv. Akad. Nauk, SSSR, Ser. Fiz. **20**, 1164 (1956), Columbia Tech. Transl. p. 1057.

[3] C. Brunnee, Z. Physik **147**, 161 (1957).

[4] Arifov, Ayukhanov, and Starodubtsev, JETP **33**, 845 (1957), Soviet Phys. JETP **6**, 653 (1958).

[5] V. I. Veksler, Dokl. Akad. Nauk Uz. S.S.R. No. 1, 9 (1956).

[6] V. I. Veksler and M. B. Ben'yaminovich, J. Tech. Phys. (U.S.S.R.) **26**, 1671 (1956), Soviet Phys.-Tech. Phys. **1**, 1626 (1957).

[7] R. E. Honig, J. Appl. Phys. **29**, 549 (1958).

[8] R. C. Bradley, J. Appl. Phys. **30**, 1 (1959).

[9] J. C. Maxwell, A Treatise of Electricity and Magnetism, Dover, 1955.

[10] N. D. Morgulis, J. Tech. Phys. (U.S.S.R.) **25**, 1667 (1955).

[11] V. I. Veksler and M. B. Ben'yaminovich, Тр. Среднеазиатского гос. ун-та (Proc. Central Asia State Univ.) **91**, 57 (1957).

[12] O. Roos, Z. Physik **147**, 184 (1957).

[13] H. Sporn, Z. Physik **112**, 278 (1939).

[14] V. I. Veksler, Izv. Akad. Nauk Uz.S.S.R. Ser. Fiz. Mat. No. 4, 34 (1959).

Translated by H. Lashinsky
78